

## Specific Heat of Normal and Superfluid $^3\text{He}^*$

T. A. Alvesalo, T. Haavasoja, and M. T. Manninen

Low Temperature Laboratory, Helsinki University of Technology, Espoo, Finland

(Received May 21, 1981)

*Extensive measurements of the heat capacity of liquid  $^3\text{He}$  in the normal and superfluid phases are reported. The experiments range from 0.8 to 10 mK and cover pressures from 0 to 32.5 bar in zero magnetic field. The phase diagram of  $^3\text{He}$ , based on the platinum NMR temperature scale, is presented. In the normal liquid at low pressures and near the superfluid transition  $T_c$  an excess specific heat is found. The effective mass  $m^*$  of  $^3\text{He}$  is at all pressures about 30% smaller than the values reported earlier. The calculated Fermi liquid parameters  $F_0$  and  $F_1$  are reduced as  $m^*/m$ , while the spin alignment factor  $(1 + Z_0/4)^{-1}$  is enhanced from 3.1–3.8 to 4.3–5.3, depending on pressure. The specific heat discontinuity  $\Delta C/C$  at  $T_c$  is for  $P = 0$  close to the BCS value 1.43, whereas at 32.5 bar  $\Delta C/C$  is  $1.90 \pm 0.03$  in the B phase and  $2.04 \pm 0.03$  in the A phase, revealing distinctly the pressure dependence of strong coupling effects. The temperature dependence of the specific heat in the B phase agrees with a model calculation of Serene and Rainer. The latent heat  $L$  at the AB transition is  $1.14 \pm 0.02 \mu\text{J/mole}$  for  $P = 32.5$  bar and decreases quickly as the polycritical point is approached; at 23.0 bar,  $L = 0.03 \pm 0.02 \mu\text{J/mole}$ .*

### 1. INTRODUCTION

The properties of normal liquid  $^3\text{He}$  can be accounted for by the Landau Fermi liquid theory<sup>1</sup> from about 100 mK down to the superfluid transition temperature  $T_c$ . This theory predicts that the specific heat of  $^3\text{He}$  is proportional to temperature. Measurements of heat capacity yield the effective mass  $m^*$  needed in the calculation of the most important Fermi liquid parameters  $F_0$ ,  $F_1$ , and  $Z_0$ . At  $T_c$  the heat capacity displays a discontinuity  $\Delta C/C$ . Data from a typical experimental run are shown in Fig. 1.

A model for the superfluid A and B phases is given by the weak coupling BCS theory extended to  $p$ -wave pairing in a spin triplet state.<sup>2</sup>

\*Work supported by the Academy of Finland.

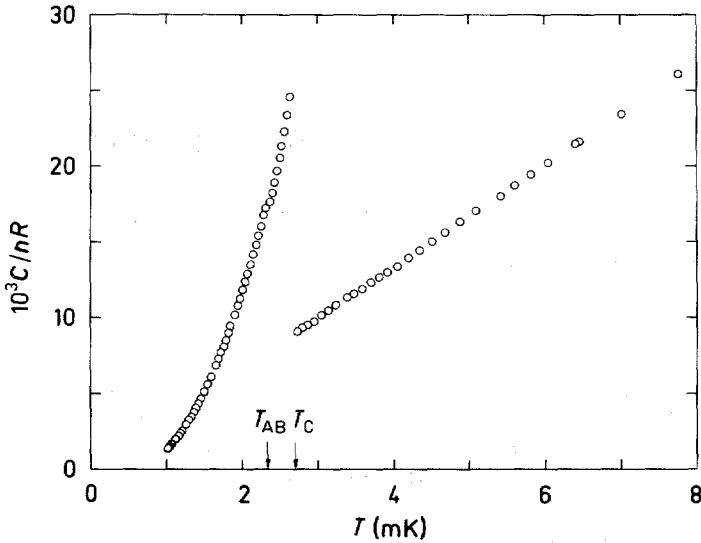


Fig. 1. Specific heat of liquid  $^3\text{He}$  vs temperature measured at  $P = 28.7$  bar in zero external magnetic field. The superfluid transition at  $T_c = 2.71$  mK and the AB transition at  $T_{AB} = 2.34$  mK are indicated by arrows.

This theory is, however, inadequate to account for the properties of superfluid  $^3\text{He}$  in quantitative detail. Deviations from the weak coupling theory are caused by residual interactions between quasiparticles; these phenomena are called strong coupling effects.<sup>2,3</sup> The temperature dependence of the specific heat below  $T_c$  and the discontinuity at  $T_c$  yield a quantitative measure of the importance of strong coupling effects.

In order to extract the relevant data, a heat capacity measurement must be sufficiently accurate. Major difficulties are due to thermometry and the background heat capacity. These are evidently the reasons why some of the previous heat capacity measurements<sup>4-9</sup> in the vicinity of  $T_c$  are rather inaccurate and inconsistent. The most reliable data are probably by Halperin *et al.*<sup>6</sup> along the melting curve.

In this paper we report extensive heat capacity measurements from 0.8 to 10 mK over the pressure range between 0 and 32.5 bar. All experiments were done in zero external magnetic field. The latent heat  $L$  of the  $B \rightarrow A$  transition was also measured. The second-order transition temperature  $T_c$  between normal liquid  $^3\text{He}$  and superfluid as well as the first-order transition temperature  $T_{AB}$  between the A and B phases was measured precisely on our temperature scale. Parts of our work have been briefly reported elsewhere.<sup>10,11</sup>

This paper contains six sections. The next section deals with experimental techniques, thermometry, and determination of the background heat capacity. Our experimental results for the normal liquid are presented in Section 3 and for the superfluid phases in Section 4. Measurements of the latent heat are described in Section 5. Conclusions from the results are summarized in the last section.

## 2. EXPERIMENTAL

### 2.1. General Techniques

Nuclear demagnetization of copper was used as our final cooling method.<sup>12</sup> The nuclear stage consists of two copper bundles, one inside the other, sharing a common magnetization field. The main superconducting magnet produces a maximum field of 7 T. Another coil was employed to eliminate the field in the experimental region to a relative accuracy better than one part in  $10^4$ . The field for the platinum NMR thermometer was produced by a third superconducting solenoid. Dilution refrigeration was used for precooling the experimental cell and the nuclear stage to about 19 mK. Thermal contact between the inner bundle and the cell was weak, so that demagnetization had to be performed slowly, in 12–24h, to reach temperatures below 1 mK. A detailed description of the cryostat and its performance with a smaller cell is given in Ref. 13.

In order to reduce the background heat capacity to a minimum the experimental cell, shown in Fig. 2, was made of silver because, like copper, it has a negligible electronic heat capacity at the temperature region of interest and, moreover, its nuclear heat capacity is two orders of magnitude smaller than that of copper. The cell can be thermally disconnected from the inner nuclear bundle by a heat switch to prevent the heat of the measuring pulses from leaking out. This heat switch was made of 66 tin wires (diameter 0.5 mm, 99.999% pure) which were soldered by indium to the silver fingers illustrated in Fig. 2.

The free volume of the experimental cell is  $17.24 \pm 0.10 \text{ cm}^3$ . Its inner parts consist of a heater, a silver sinter of surface area  $\sim 10 \text{ m}^2$ , and two thermometers based on platinum NMR and on the susceptibility of cerium magnesium nitrate diluted by the corresponding lanthanum salt (CLMN). The heater was made of 6 m of bifilarly wound silver wire (0.07 mm in diameter).

Sealing of the cell was done by indium soldering between the main chamber and its support, and between the CLMN thermometer appendage and its cover. The tube connecting the appendage to the cell was silver soldered at both ends. All joints were made with the smallest possible

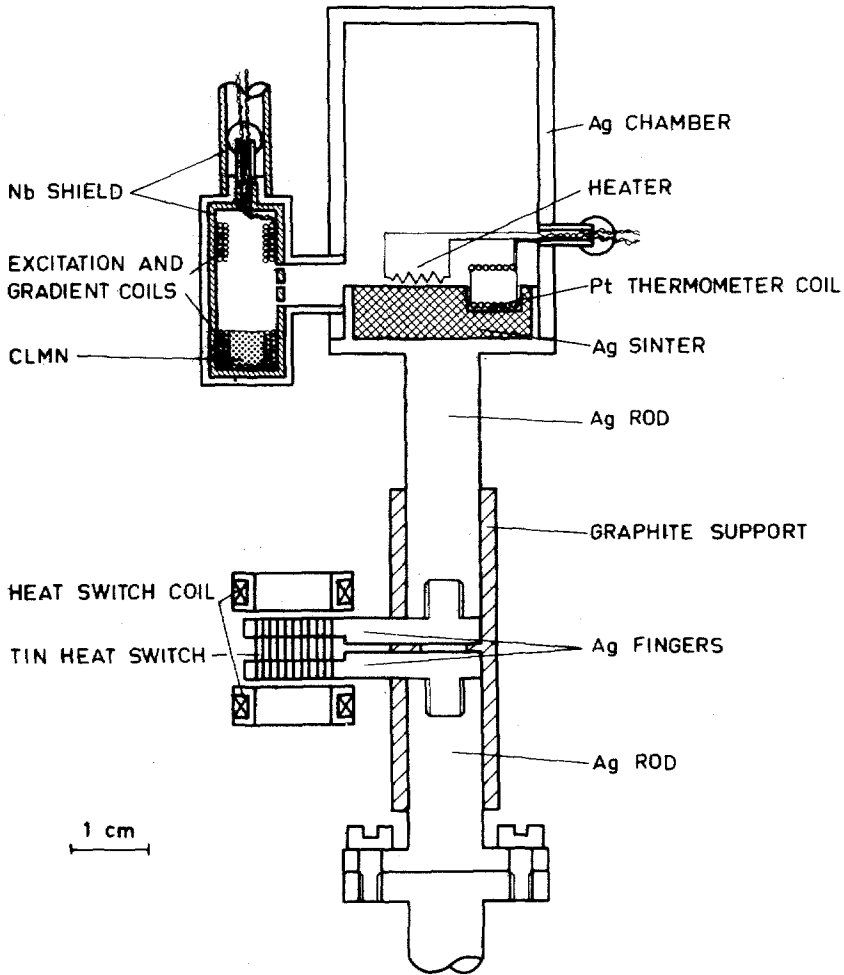


Fig. 2. The experimental cell.

amount of indium solder in order to avoid excessive background heat capacity. The large quadrupolar heat capacity of indium is not present in the superconducting state.<sup>14</sup> The electrical feedthroughs were sealed by epoxy.

Pressure on the experimental cell was measured through a filling capillary by a quartz Bourdon gauge, calibrated with a dead weight tester to an accuracy of 0.1%. The resolution of the gauge is about 2 mbar. Stabilization of the pressure was achieved by means of a feedback system,

which uses the error signal from the gauge to operate a heater on a  $50\text{ cm}^3$  volume at room temperature connected to the  $^3\text{He}$  cell. The sample pressure was stable within 10 mbar, except when transferring liquid  $^4\text{He}$  to the dewar. After a transfer the pressure regained its value in 15 min.

To obtain pressures above the melting curve minimum the dilution refrigerator and the cell were first warmed to  $T \geq 1\text{ K}$ . The cell was then pressurized so that the molar volume corresponded to the desired liquid pressure at temperatures below the melting curve minimum. We have employed the molar volume data of Grilly<sup>15</sup> and estimate an accuracy of  $\pm 0.3$  bar.

The  $^3\text{He}$  gas was purified by means of a rectification column similar to that of Grigor'ev *et al.*<sup>16</sup>; the  $^4\text{He}$  content was measured to be about 10 ppm in room temperature gas.

## 2.2. Measurement of Heat Capacity

Heat capacities were measured with the pulse technique: A small amount of heat  $\Delta Q$  was electrically applied to the sample and the corresponding increase in temperature  $\Delta T$  was measured. The heat capacity  $C$  may then be calculated from  $C = \Delta Q/\Delta T$ . In a separate experiment the resistance  $R_h$  of the silver heater wire was found by the four-lead method to be  $R_h = 1.013 \pm 0.002\ \Omega$ . The length of a heat pulse was typically 30 sec. The accuracy of our measurements of  $\Delta Q$  was estimated to be 0.3%. Changing the current and length of the pulse over broad limits did not cause additional scatter in the data.

After demagnetization, when  $^3\text{He}$  had reached its lowest temperature, the current in the heat switch coil was reduced to make the switch nonconducting. This caused the sample to warm from below 0.7 mK to 0.8 mK at zero pressure, corresponding to a heat pulse of  $1.2\ \mu\text{J}$ . This amount of heat is likely to be due to the magnetic energy of the switch, since the calculated eddy current heating is negligible. Generally the heat leak to the sample was less than 0.1 nW. At zero pressure this corresponds to a warmup rate of  $\dot{T} < 10\text{ nK/sec}$  for a full cell above  $T_c$ .

The temperature and its change  $\Delta T$  for a heat capacity point were determined by extrapolating the initial and final warmup slopes to the middle of pulse to find  $T_i$  and  $T_f$ , respectively; then  $T = \frac{1}{2}(T_i + T_f)$ ,  $\Delta T = T_f - T_i$ . The precision of the extrapolation was usually better than 1%, and it is the principal cause for the scatter in the data. Heat pulses were selected so that  $\Delta T/T$  was between 0.01 and 0.04.

A typical response of the CLMN thermometer to a heat pulse is shown in Fig. 3. The length of the pulse was 30 sec. At  $T \geq 5\text{ mK}$  the relaxation time for the temperature after the pulse was proportional to  $T^2$ , as one

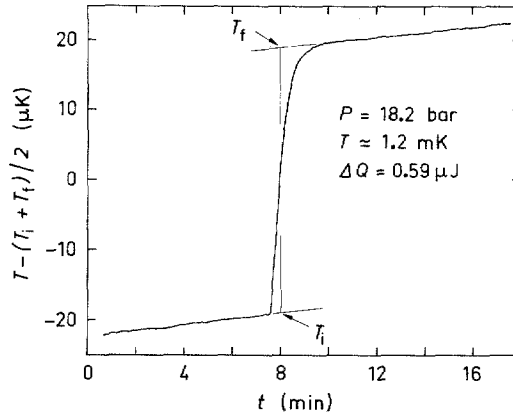


Fig. 3. A typical response of the CLMN thermometer to a heat pulse. Determination of initial and final temperatures  $T_i$  and  $T_f$ , respectively, is shown by the straight lines. Heat was on 30 sec.

would expect for a normal Fermi liquid, since the heat capacity behaves like  $C \propto T$  and the heat conductivity like  $K \propto T^{-1}$ . At lower temperatures the relaxation time saturated to about 40 sec; this is presumably due to a time constant related to the CLMN pill. Consequently, we did not observe any possible difference between the relaxation times of the superfluids and normal  $^3\text{He}$ .

### 2.3. Thermometry and the Temperature Scale

For platinum NMR thermometry we have employed the commercial pulse gating and signal processing unit PLM3,\* based on the technique described in Ref. 17. The nuclear magnetic susceptibility of platinum is assumed to obey the Curie law  $\chi \propto 1/T$ . The constant of proportionality was found by measuring the spin-lattice relaxation time  $\tau_1$  and by using the Korringa relation  $\tau_1 T = 29.9$  msec K valid for platinum at 28 mT.<sup>18,13</sup>

A temperature dependence of the Korringa relation has been observed in some laboratories.<sup>19,20</sup> In order to check the validity of this relation for our platinum powder we have plotted  $\tau_1 T$  vs  $T$  in Fig. 4. Temperatures were determined by the susceptibility measurements, which were calibrated by taking the average  $\langle \tau_1 T \rangle$  to be 29.9 msec K. There is no evident temperature dependence in  $\tau_1 T$  within the precision of our  $\tau_1$  measurements, about 2%. Typically  $\tau_1$  was measured in a temperature region from 2 to 10 mK. Below 2 mK the thermal contact between the platinum powder

\*PLM-3 platinum NMR thermometer, Instruments for Technology, Espoo, Finland.

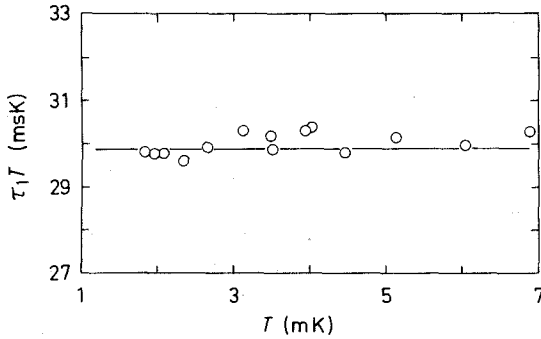


Fig. 4. A plot of  $\tau_1 T$  vs the Curie temperature of the platinum thermometer. The Curie constant was calibrated so that, on the average,  $\tau_1 T = 29.9$  msec K. A single point is an average of three  $\tau_1$  measurements.

and  $^3\text{He}$  seems to become poor. At high temperatures the NMR signal is reduced and the measurement becomes more susceptible to systematic errors. This can, in principle, be avoided by increasing the tipping angle of the platinum spins after a pulse. In practice, however, an analysis of  $\tau_1$  measurements is problematic when large tipping angles are employed.

The platinum NMR thermometer is not precise enough for accurate heat capacity measurements. Therefore, we used a CLMN thermometer similar to that of Paulson *et al.*<sup>21</sup>; we diluted our cerium magnesium nitrate [ $\text{Ce}_2\text{Mg}_3(\text{NO}_3)_{12} \cdot 24\text{H}_2\text{O}$ ] to 3 molar percent ( $\text{Ce}_{0.03}\text{La}_{0.97}\text{MN}$ ) in the corresponding lanthanum salt. The preparation of the salt and the thermometer coils are described in Ref. 11. The magnetization of CLMN was monitored by an ac bridge\* working at 32 Hz and using a SQUID† as a null detector. The output showing the off-balance of the bridge was lock-in detected and recorded on a chart. We obtained a resolution of better than one part in  $10^4$  below 10 mK.

The CLMN thermometer was calibrated against the nuclear spin susceptibility of platinum in every cooldown. A useful empirical relation for the CLMN bridge output  $S$  is

$$S = \frac{A}{T - \Delta} + S_0 \quad (1)$$

where  $S_0$  is a temperature-independent signal,  $T$  is the absolute temperature, and  $A$  and  $\Delta$  are calibration constants. Using the Curie law for

\*RLM Measuring System, S.H.E. Corporation, San Diego, California.

†SUM3 Magnetometer, Instruments for Technology, Espoo, Finland.

the integrated platinum NMR signal

$$S_{\text{Pt}} = B/T \quad (2)$$

and by plotting  $(S - S_0)^{-1}$  vs  $S_{\text{Pt}}^{-1}$ , one would thus expect a linear dependence with the slope  $B/A$  and intercept  $-\Delta/A$ , where the calibration constant  $B$  is determined from  $\tau_1$  measurements. Such a plot is shown in Fig. 5, where  $S_{\text{Pt}}^{-1}$  is replaced by  $T$  for the sake of convenience. This analysis yielded negative values for  $\Delta$ , ranging for different cooldowns between  $-0.11$  and  $-0.13$  mK with the earth's field compensated. The parameter  $A$  was found to be constant to within 1%. Calibrations did not indicate any pressure dependence within the precision of our  $\tau_1$  measurements and the value of  $S$  at  $T_c$  was field independent at least up to 28 mT. Due to the imprecision of the  $\tau_1$  measurements we have fixed the temperature scale so that at zero pressure  $T_c = 1.040$  mK, an average value of different calibrations.

The absolute accuracy of our temperature scale relies on the precision of the  $\tau_1$  measurements and on the value of the Korringa constant  $K_{\text{Pt}}$  in platinum. There are several reported measurements on  $K_{\text{Pt}}$ .<sup>22,23,18</sup> Aalto *et al.*<sup>22</sup> have verified the validity of the Korringa relation from 10 mK to

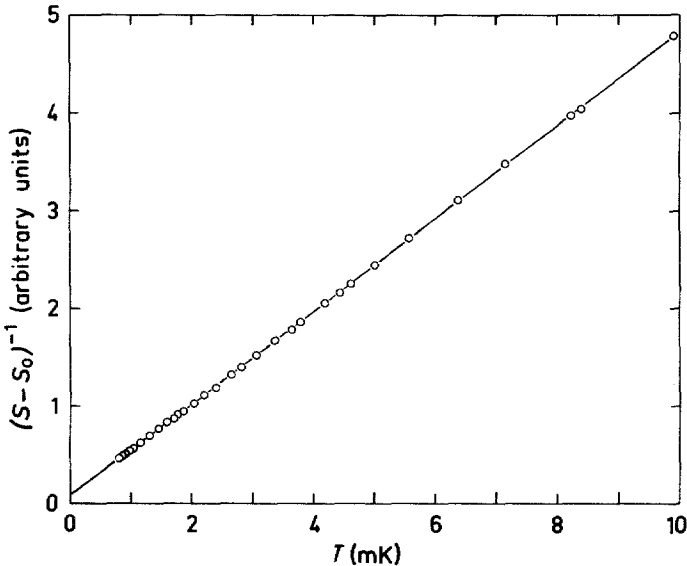


Fig. 5. The inverse of the temperature-dependent magnetometer signal  $(S - S_0)^{-1}$  vs the Curie temperature of the platinum thermometer. The parameters  $A$  and  $\Delta$  are determined by the inverted slope of the straight line and by the intercept at the temperature axis, respectively.

1 K and find  $K_{\text{Pt}} = 29.6$  msec K, in agreement with the earlier reported measurements at higher temperatures. Their temperature scale was based on a CMN thermometer and on a carbon resistor calibrated against the vapor pressure of  $^3\text{He}$ . At the low-temperature end they further employed a nuclear orientation (NO) thermometer with  $^{54}\text{Mn}$  in nickel.<sup>24</sup> The stated absolute accuracy of the NO thermometer is 2%.

Ahonen *et al.*<sup>18</sup> measured  $K_{\text{Pt}}$  with 1% precision between 7 and 35 mK using a similar NO thermometer as Aalto *et al.*<sup>22</sup> and they report  $K_{\text{Pt}} = 29.9 \pm 0.3$  msec K, which is the value adopted here. Avenel *et al.*<sup>23</sup> have measured  $K_{\text{Pt}}$  using an osmotic pressure thermometer from 50 mK to 2 K and they obtained  $K_{\text{Pt}} = 30.2$  msec K. Their precision is about 1% and the absolute accuracy of the thermometer is 2 mK at  $T > 50$  mK. On the basis of the above measurements and the precision of the  $\tau_1$  measurements we estimate the absolute accuracy of our temperature scale to be  $\pm 5\%$ .

The phase diagram of  $^3\text{He}$  is shown in Fig. 6 on our temperature scale; the experimental points are listed in Table I. The  $T_c$  was observed as a change in the slope of the temperature vs time curve and  $T_{\text{AB}}$  as a plateau when drifting from the B to the A phase. At several pressures  $T_c$  was

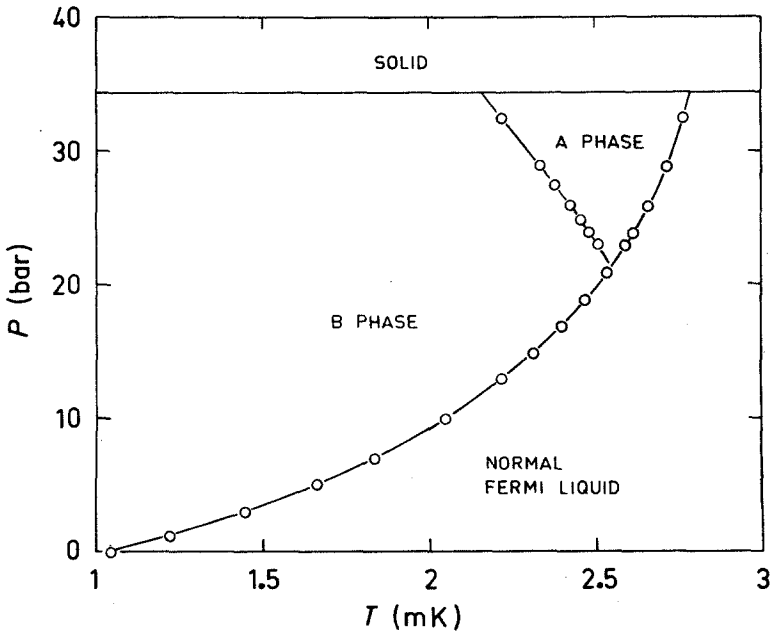


Fig. 6. The phase diagram of liquid  $^3\text{He}$  in zero magnetic field. The phase transitions at  $T_c$  and  $T_{\text{AB}}$  were determined by the CLMN thermometer, which was calibrated against the platinum thermometer using the Korringa relation  $\tau_1 T = 29.9$  msec K.

TABLE I

Pressure and Temperature Coordinates of the  $T_c$  and  $T_{AB}$  Lines in Zero Magnetic Field

| $P$ , bar | $T_c$ , mK | $P$ , bar         | $T_c$ , mK         | $P$ , bar         | $T_{AB}$ , mK      |
|-----------|------------|-------------------|--------------------|-------------------|--------------------|
| 0         | 1.040      | 16.94             | 2.400              | 23.01             | 2.512              |
| 1.186     | 1.220      | 18.93             | 2.472              | 23.97             | 2.484              |
| 2.966     | 1.446      | 20.98             | 2.538              | 24.88             | 2.459              |
| 5.032     | 1.663      | 23.01             | 2.595              | 25.96             | 2.426              |
| 6.976     | 1.834      | 23.95             | 2.618 <sup>a</sup> | 27.46             | 2.381              |
| 9.951     | 2.048      | 25.94             | 2.662 <sup>a</sup> | 28.96             | 2.335              |
| 12.93     | 2.217      | 28.95             | 2.719              | 32.5 <sup>b</sup> | 2.221 <sup>a</sup> |
| 14.91     | 2.314      | 32.5 <sup>b</sup> | 2.768 <sup>a</sup> |                   |                    |

<sup>a</sup>Except for these data, only a single calibration of the thermometer was used.<sup>b</sup>The pressure  $32.5 \pm 0.03$  bar was estimated using the molar volume data of Grilly.<sup>15</sup>

detected during both cooling and warming; a difference of  $\sim 0.5 \mu\text{K}$  was observed with  $\dot{T} \sim 20 \text{ nK/sec}$ . With lower drift rates the difference was reduced and, in general, reproducibility within our resolution could be achieved during a single cooldown. The  $A \rightarrow B$  transition was supercooled, but in the reversed direction  $B \rightarrow A$  the transition temperature was reproducible within  $1 \mu\text{K}$  and constant within  $0.5 \mu\text{K}$  during the transition.

It is interesting to compare the recent La Jolla temperature scale<sup>21</sup> to ours. We made a polynomial fit to the magnetic temperature data of Ref. 21 (here  $T_{LJ}^*$ ) vs pressure in order to compare them with our  $T_c$  data ( $T_{Hki}$ ). It was found that the two temperature scales depend linearly on each other. A least squares fit yields

$$T_{LJ}^* = 0.900T_{Hki} + 0.114 \text{ mK} \quad (3)$$

This relation is valid within  $5 \mu\text{K}$ , as can be seen from Fig. 7. One may infer from this figure that deviations from Eq. (3) are not caused by experimental scatter, which seems to be less than  $1 \mu\text{K}$ . Near zero pressure an error of 25 mbar corresponds to an error of  $5 \mu\text{K}$  in  $T_c$ . However, we find such a pressure inaccuracy improbable.

Equation (1) can be cast into the form  $T = T^* + \Delta$ , where  $T^* = A/(S - S_0)$  is the magnetic temperature. Using  $T_{Hki}^*$  in Eq. (3), we obtain  $T_{LJ}^* = 0.900T_{Hki}^* + 0.003 \text{ mK}$ . This means that with high precision  $T_{LJ}^* \propto T_{Hki}^*$  and consequently the  $\Delta$  parameters of the La Jolla and Helsinki thermometers must be equal within the factor of proportionality, 0.9, and the precision of the result. This conclusion is actually independent of our calibration procedure. However, the value of  $\Delta$  found by Paulson *et al.*<sup>21</sup> is  $+0.1 \text{ mK}$ , in contradiction to our measurement,  $\Delta \approx -0.12 \text{ mK}$ . Their value of  $\Delta$  is only an estimate, which makes zero-sound attenuation linear in  $T^2$  at temperatures well above  $T_c$ . The sign of  $\Delta$  in our measurements

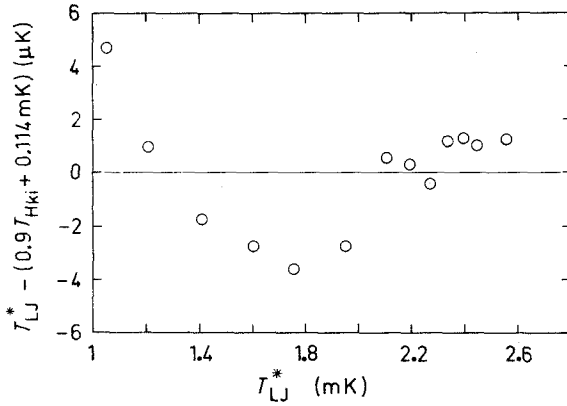


Fig. 7. A comparison of the Helsinki and La Jolla temperature scales. The quantity  $T_{LJ}^* - (0.900 T_{Hki} + 0.114 \text{ mK})$  is displayed vs  $T_{LJ}^*$ .

depends solely on the validity of the Curie law for the static nuclear spin susceptibility. A negative  $\Delta$  would affect considerably the discussion of Ref. 21 concerning earlier work.

Experiments by Halperin *et al.*<sup>25</sup> at the melting curve yielded  $T_c = 2.75 \pm 0.11 \text{ mK}$  and  $T_{AB} = 2.18 \pm 0.10 \text{ mK}$ . Their temperature scale was determined in two steps. First, a scale proportional to the thermodynamic temperature was derived by measuring the latent heat for converting liquid to solid and by applying the Clausius–Clapeyron equation.  $T_c$  is used as a well-defined reference temperature on this scale. In the second step, the value of  $T_c$  was determined by using the fact that the solid entropy approaches  $R \ln 2$  at sufficiently high temperatures. Their results on this absolute thermodynamic temperature scale are in good agreement with our extrapolated values,  $T_c = 2.79 \text{ mK}$  and  $T_{AB} = 2.16 \pm 0.02 \text{ mK}$ ; here the error limits represent the precision of extrapolation.

Direct check of our temperature scale was recently made by Lhota *et al.*<sup>26</sup> In this experiment the Helsinki scale was produced with the help of the platinum susceptibility; the superfluid transition temperature  $T_c = 1.04 \text{ mK}$  of  $^3\text{He}$  at zero pressure was used to determine the Curie constant. This scale was compared with the NBS cryogenic temperature scale,<sup>27</sup> whose accuracy between 10 and 50 mK is  $\pm 0.5\%$ , by means of tungsten and beryllium superconductive fixed points. According to these measurements, the value of  $T_c$  at zero pressure is  $1.025 \pm 0.02 \text{ mK}$  on the NBS scale, in good agreement with our  $T_c$ . This result, as well as the consistency of the data of Ref. 25 with our values of  $T_c$  at the melting curve, give convincing support for the correctness of our temperature scale. The  $T_c$

line according to the old Helsinki scale,<sup>18</sup> based also on platinum NMR, is at 2% higher temperatures than ours, on the average.

#### 2.4. Determination of the Background Heat Capacity

It is not possible to measure the background heat capacity of the empty cell directly, owing to inadequate thermal contact between the CLMN thermometer and the rest of the cell. Further, since our intention was to measure the specific heat of bulk liquid, a possible contribution from the sinter must be properly taken into account. The first layer(s) of solid  $^3\text{He}$  at surfaces, for example, may have a substantial heat capacity. Also, superfluidity is prohibited near surfaces to within the superfluid coherence length  $\xi_0$ .

At zero pressure one can eliminate the background and nonbulk liquid contributions by measuring, in turn, the heat capacities of a partially filled and a full cell. The difference in the measured heat capacities is due to the different amounts of bulk  $^3\text{He}$  in the two experiments, assuming that the liquid level was well above the sinter with partial filling. In order to improve our accuracy, we have extended this technique by measuring the heat capacity with 15 different amounts of liquid  $^3\text{He}$  in the cell at zero pressure. Plotting the measured heat capacity  $C_m$  at a given temperature  $T \geq T_c$  vs the volume  $V$  of liquid  $^3\text{He}$  in the cell, one expects to find a straight line

$$C_m(T, V) = c_n(T)V + C_b(T) \quad (4)$$

where the slope  $c_n(T)$  is the heat capacity of normal liquid  $^3\text{He}$  per unit volume and the intercept  $C_b(T)$  contains all background and nonbulk liquid contributions at this temperature. Such a graph is displayed in Fig. 8 at  $T = 1.1$  mK.

We have measured  $V$  from the volume of  $^3\text{He}$  gas condensed to the cell. Some of this gas remains as liquid in the gravitational minima of the filling capillary, which has a volume of only  $0.08 \text{ cm}^3$  below the still of the dilution refrigerator. The amount of liquid in the filling capillary has been deduced by requiring that  $C_m \propto V$  at  $T \geq 8$  mK, where the background has become negligible. This implies a correction of  $0.06 \text{ cm}^3$  to  $V$ , which is consistent with the volume of the filling capillary.

The intercepts of the straight lines of Eq. (4) at  $V = 0$  are presented as a function of temperature in Fig. 9. The drop of about 20% at  $T_c$  can be interpreted as suppression of superfluidity within  $\xi_0$  on the surfaces and will be discussed below. The  $V = 0$  intercept in the normal liquid  $^3\text{He}$  yields a background contribution which satisfactorily obeys the empirical relationship

$$C_b(T) = 2.55e^{-T/2.3} \text{ mJ/K} \quad (5)$$

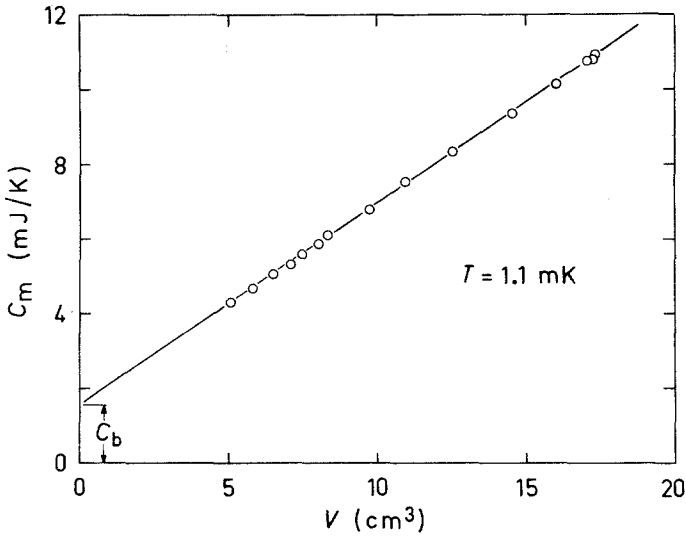


Fig. 8. The measured heat capacity  $C_m$  vs the  $^3\text{He}$  sample volume  $V$  at constant  $T$  at zero pressure. The slope of the straight line yields the specific heat, and the intercept at  $V=0$  yields the background heat capacity  $C_b$ .

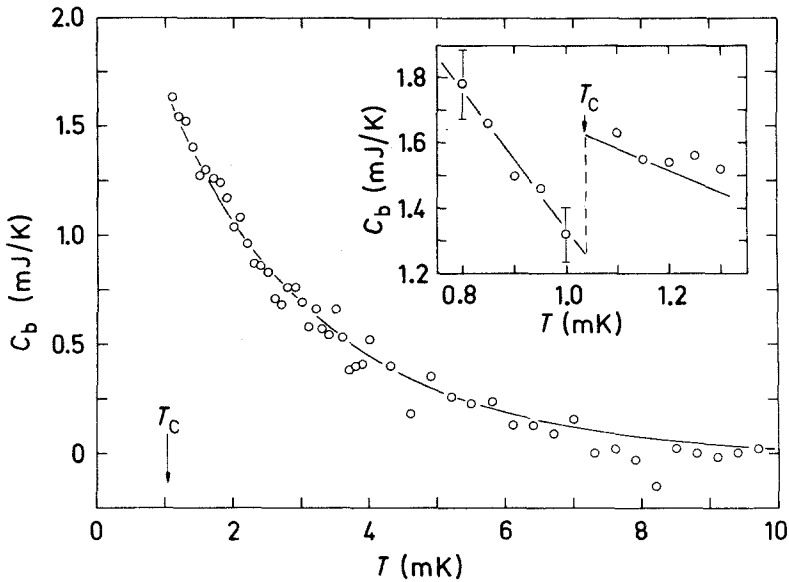


Fig. 9. The background heat capacity  $C_b(T)$  as determined from Eqs. (4) and (6). The solid line above  $T_c$  follows Eq. (5). At  $T_c(P=0) = 1.04$  mK there is a drop of about 20% in  $C_b(T)$ , as shown by the dashed line in the inset. This is taken to be due to suppression of superfluidity at surfaces of the sinter.

where  $T$  is in mK. At  $T_c = 1.04$  mK we find  $C_b = 1.62 \pm 0.05$  mJ/K, which amounts to about 15% of the heat capacity of the cell full of normal liquid  $^3\text{He}$  at  $P = 0$ . A background of this size can be accounted for by assuming the validity of a  $T^{-2}$  dependence<sup>28</sup> for the specific heat of solid  $^3\text{He}$  down to 1 mK and by further assuming that the first layer of solid at surfaces exhibits a heat capacity not much different from that of bulk solid. If some of the indium used in soldering the tin wires in the heat switch is in the normal state, we estimate the nuclear quadrupole heat capacity of indium<sup>14</sup> to contribute only 0.2 mJ/K at 1 mK.

If a volume  $V_n$  of liquid  $^3\text{He}$  remains normal below  $T_c$ , Eq. (4) should be replaced by

$$\begin{aligned} C_m(T, V) &= c_s(T)V_s + c_n(T)V_n + C'_b(T) \\ &= c_s(T)V + [c_n(T) - c_s(T)]V_n + C'_b(T) \end{aligned} \quad (6)$$

where  $V = V_s + V_n$  and the subscripts  $s$  and  $n$  refer to superfluid and normal liquid, respectively. The intercept  $C_b$  at  $V = 0$  is now described by the two extreme terms on the right in the latter form of Eq. (6), where  $C'_b(T)$  corresponds to  $C_b(T)$  in Eq. (5). The drop in  $C_b$  at  $T_c$ , as shown in Fig. 9, can be understood on the basis of the middle term in Eq. (6), since  $c_n < c_s$  just below  $T_c$ . Estimating the amount of normal liquid below  $T_c$  from Eq. (6), we find  $V_n = 0.50 \pm 0.05$  cm<sup>3</sup>. This would correspond to a 50-nm-thick layer of normal liquid on the sinter surface. This value is roughly of the same magnitude as the temperature-independent coherence length<sup>2</sup>  $\xi_0 = \hbar v_F / \pi k_B T_c$ . Contributions from the term  $(c_n - c_s)V_n$  vanish for the temperature  $T/T_c \approx 0.5$  where, assuming that  $c_n \propto T$ ,  $c_n$  and  $c_s$  become equal (cf. Fig. 1). This interpretation is consistent with the temperature dependence shown in Fig. 9.

Since there is no direct way of measuring the background heat capacity at finite pressures, we have simply taken  $C_b(T)$  to be pressure independent. If  $C_b(T)$  is, in fact, due to formation of solid  $^3\text{He}$  or to the presence of high-pressure liquid at the sinter surface, it could have a weak pressure dependence. The background, however, is so small that our assumption is quite reasonable.

The pressure dependence of  $V_n$  below  $T_c$  can be estimated from the coherence length. One finds

$$\xi_0 = \frac{\hbar v_F}{\pi k_B T_c} \propto \frac{(V/n)^{1/3}}{\gamma T_c} \quad (7)$$

where  $V/n$  is the molar volume and  $\gamma$  is a constant defined by  $C_n/nR = \gamma T$ . Here  $n$  is the number of moles and  $R$  is the gas constant. All pressure

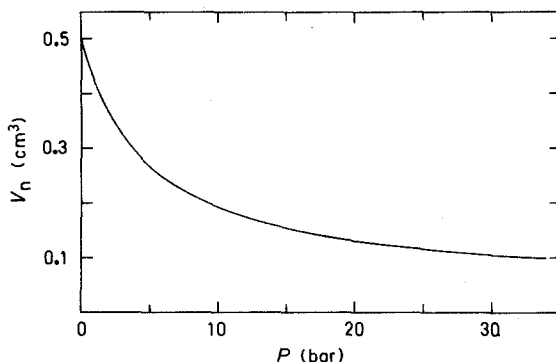


Fig. 10. The estimated normal fraction  $V_n$  below  $T_c$  in the sinter as a function of pressure:  $V_n(P) = V_n(0)\xi_0(P)/\xi_0(0)$ .

dependent terms in Eq. (7) tend to decrease  $\xi_0$  with increasing  $P$ . In Fig. 10 we have plotted  $V_n$ , scaled by  $\xi_0$ , as a function of pressure. At  $T_c$  the correction in  $c_s$  due to  $V_n$  is +1.7% at 0 bar and less than 1% at  $P > 5$  bar.

To summarize, in the normal liquid region we have assumed that  $C_b$  is independent of pressure and we have subtracted from the measured heat capacity a background given by Eq. (5). Below  $T_c$  the effect of normal  $^3\text{He}$  near sinter surfaces is taken into account according to the measurements at  $P = 0$ . Any systematic errors due to the above procedures are estimated to be less than 1% in heat capacity.

### 3. SPECIFIC HEAT OF NORMAL LIQUID $^3\text{He}$

#### 3.1. Results

The specific heat of a normal Fermi liquid is proportional to  $T$ , and the quantity  $\gamma = C/nRT$  consequently depends only on pressure in the low-temperature limit. In Fig. 11 we have plotted  $\gamma$  vs  $T$  at various pressures. Roughly above 3 mK,  $\gamma$  seems to exhibit no temperature dependence. However, at temperatures below 3 mK and at pressures  $P \leq 8$  bar,  $C/nRT$  starts to increase toward  $T_c$ . The excess specific heat is most prominent at zero pressure, where the increase in  $C/nRT$  amounts to 9% at  $T_c$ . At 8 bar an upturn can hardly be resolved any more.

Let us introduce the quantity  $\Delta\gamma$  through

$$\Delta\gamma(P, T) = C/nRT - \gamma(P) \quad (8)$$

Here  $\gamma(P)$  is experimentally determined in the temperature region where  $C/nRT$  depends only on pressure. If  $\Delta\gamma$  were due to an error  $\Delta C_b$  in the

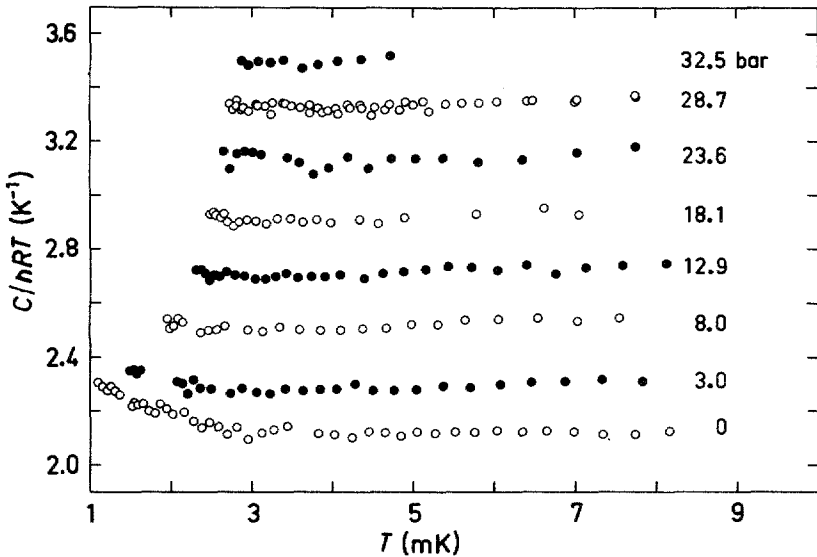


Fig. 11.  $C/nRT$  vs temperature at various pressures.

background heat capacity, that is,  $\Delta\gamma = \Delta C_b/nRT$ , then at a given temperature  $T_0$  the ratio of  $\Delta\gamma$ 's from two different pressures ought to be that of the corresponding molar volumes, assuming that  $C_b$  is independent of pressure. However,  $\Delta\gamma(P, T_0)$  seems to vanish faster than expected for increasing pressure. If the temperature scale were nonlinear, one would have  $\Delta\gamma(P, T_0) \propto \gamma(P)$  and  $\Delta\gamma$  would increase at higher pressures, which is not the case. Furthermore, a nonlinearity in the CLMN thermometer would show up in the calibration against the nuclear susceptibility of platinum. We may therefore conclude that the excess specific heat is a physical property of  $^3\text{He}$  and not of experimental origin.

In principle, the excess specific heat can either be a property of the bulk liquid or a surface effect.<sup>29</sup> Owing to our method of determining the background heat capacity, any surface contribution from the sinter is included in  $C_b$ . Therefore, the only surfaces that could cause the excess in  $C/nRT$  are the cell walls above the sinter. Let us assume that the total background is caused by sinter surfaces. If the excess were caused by the cell walls, all liquid within the sinter should be influenced by the same surface effect, since otherwise the amounts of the excess and background heat capacities could not scale in the measured ratio  $\sim 1/2$ . In this case the characteristic length for the surface effect, estimated from the volume of liquid inside the sinter ( $\sim 2 \text{ cm}^3$ ), would be a few hundred micrometers.

This is much longer than the quasiparticle mean free path in liquid  $^3\text{He}$  or the range of surface potentials. Furthermore,  $\Delta\gamma$  has a steeper temperature dependence than  $C_b$ . If only a fraction of  $C_b$  were caused by surface effects, the required characteristic length would still increase.

The above considerations seem to suggest that the excess specific heat is a property of bulk liquid  $^3\text{He}$ . Unfortunately, there is no obvious physical model predicting such an effect. The spin fluctuation theories,<sup>30-32</sup> which at the lowest temperatures yield a term  $T^3 \ln T$  to the specific heat, cannot be fitted to our data.

Evidence for anomalous effects in  $^3\text{He}$  near the superfluid transition have been reported earlier.<sup>5,8,33</sup> However, the anomaly in the heat capacity data of Dundon *et al.*<sup>5</sup> is not probably mainly due to the sinter surfaces of the cell, which do not contribute at all in our measurements. Parpia *et al.*<sup>33</sup> have observed a deviation from the  $T^{-2}$  dependence in viscosity below 4 mK. This may be due to the fact that the quasiparticle mean free path becomes comparable to their viscometer dimensions at low temperatures. However, a theoretical estimate by Jaffe<sup>34</sup> does not support this interpretation; the observed effect appears to be too large by an order of magnitude.

The effective mass  $m^*$  of liquid  $^3\text{He}$  and the Fermi liquid parameter  $F_1$  can be calculated directly from our  $\gamma(P)$  values using the known molar volumes  $V/n$ .<sup>1,35</sup> We have determined  $\gamma(P)$  as the average of our  $C/nRT$  data in the region where no excess heat capacity was observed. Our values of  $\gamma$  are plotted vs  $P$  in Fig. 12 and listed in Table II. For pressures above 8 bar,  $\gamma$  varies linearly with  $P$  within the precision of our data. The smoothed and extrapolated  $\gamma$ 's and the values of parameters  $m^*/m$ ,  $F_0$ ,  $F_1$ , and  $Z_0$  are listed in Table III. In the calculation we have used the molar volume, first-sound, and magnetic temperature data of Ref. 35.

A striking feature of our results is that the  $\gamma$ 's compiled by Wheatley<sup>35</sup> are roughly 40% larger than ours and, consequently, the Fermi liquid parameters in Table III differ considerably from those of Ref. 35. Most of this discrepancy is likely to be due to different temperature scales. For example, if the scales were related as in Eq. (3), at high temperatures a correction by the factor  $(0.9)^2$  should be applied to the  $\gamma$ 's of Ref. 35 for a comparison with our data; the discrepancy would then reduce to 15%. Unfortunately, the absolute accuracy of the low-temperature scales is not known. This leaves considerable inexactness to the Fermi liquid parameters, however precise the measurements of heat capacity are.

If we scale our values of  $\gamma$  so that they coincide with those of Ref. 35 at  $P = 0$ , we can compare the relative pressure dependence of these two sets of data. One then finds that the pressure dependence is the same up to 18 bar within 1%. Above this pressure our  $\gamma$ 's increase more quickly; at 32.5 bar our scaled  $\gamma$  is 4% larger.

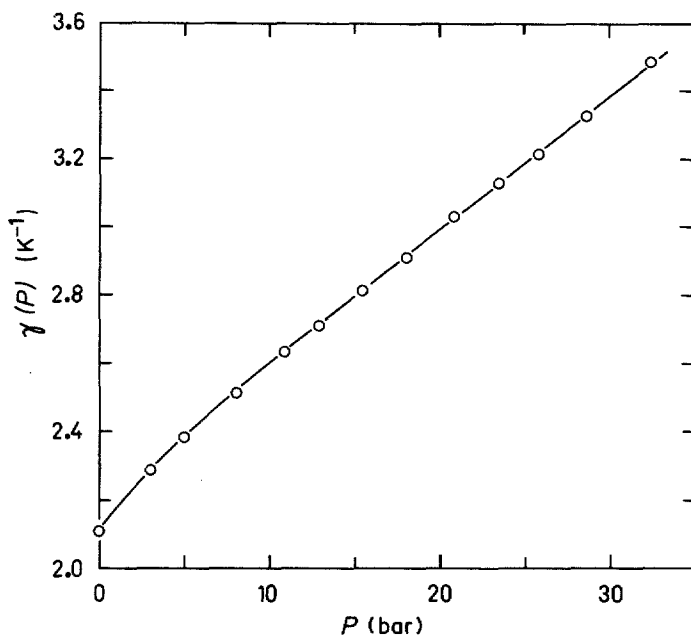


Fig. 12. The averaged  $C/nRT$  data vs pressure. The region of the excess specific heat has been excluded. The solid line follows the smoothed data of Table III.

TABLE II

The Averaged  $\gamma = C/nRT$  Values at Our Experimental Pressures<sup>a</sup>

| $P$ , bar | $\gamma$ , $K^{-1}$ | $P$ , bar         | $\gamma$ , $K^{-1}$ |
|-----------|---------------------|-------------------|---------------------|
| 0         | 2.11                | 18.10             | 2.91                |
| 3.00      | 2.29                | 20.94             | 3.03                |
| 4.99      | 2.39                | 23.59             | 3.13                |
| 8.02      | 2.51                | 25.94             | 3.21                |
| 10.94     | 2.64                | 28.66             | 3.33                |
| 12.92     | 2.71                | 32.5 <sup>b</sup> | 3.49                |
| 15.44     | 2.81                |                   |                     |

<sup>a</sup>The region of the excess specific heat was excluded when calculating the average.

<sup>b</sup>The pressure  $32.5 \pm 0.03$  bar was estimated using the molar volume data of Grilly.<sup>15</sup>

**TABLE III**  
Smoothed Values of  $\gamma$ ,  $m^*/m$ ,  $F_0$ ,  $F_1$ , and  $Z_0$  vs Pressure.<sup>a</sup>

| $P$ , bar          | $\gamma$ , $\text{K}^{-1}$ | $m^*/m$ | $F_0$ | $F_1$ | $Z_0$ |
|--------------------|----------------------------|---------|-------|-------|-------|
| 0                  | 2.11                       | 2.12    | 6.78  | 3.36  | -3.08 |
| 3                  | 2.29                       | 2.43    | 12.0  | 4.28  | -3.15 |
| 6                  | 2.43                       | 2.68    | 17.1  | 5.03  | -3.18 |
| 9                  | 2.56                       | 2.90    | 22.1  | 5.69  | -3.20 |
| 12                 | 2.68                       | 3.10    | 27.0  | 6.31  | -3.23 |
| 15                 | 2.80                       | 3.30    | 32.0  | 6.91  | -3.24 |
| 18                 | 2.91                       | 3.50    | 37.2  | 7.51  | -3.25 |
| 21                 | 3.03                       | 3.69    | 42.4  | 8.08  | -3.25 |
| 24                 | 3.14                       | 3.88    | 47.8  | 8.64  | -3.24 |
| 27                 | 3.26                       | 4.07    | 53.5  | 9.21  | -3.24 |
| 30                 | 3.38                       | 4.27    | 59.5  | 9.80  | -3.24 |
| 33                 | 3.50                       | 4.47    | 65.8  | 10.41 | -3.24 |
| 34.36 <sup>b</sup> | 3.56                       | 4.56    | 68.7  | 10.68 | -3.23 |

<sup>a</sup>The experimental data on molar volume, first sound, and magnetic temperature needed to calculate these parameters are from Ref. 35.

<sup>b</sup>The results at this pressure are extrapolated from smoothed data at lower pressures.

The discrepancy in the relative pressure dependence of the  $\gamma$ 's could be attributed to a small background contribution on the heat capacity data of Abel *et al.*,<sup>36</sup> on which the  $\gamma$ 's of Ref. 35 are mainly based. Comparing with our data, one can show that a 7% contribution from the background to the  $P = 0$  heat capacity of  $^3\text{He}$  is enough to cause the discrepancy. The measurements of Abel *et al.* were made by the difference method: first the total heat capacity was measured with a small free volume filled by  $^3\text{He}$  and then with an enlarged volume, so that the difference in the heat capacity was due to the extra bulk  $^3\text{He}$ . Since the total heat capacity was at 8 mK, roughly twice as large as that due to the extra bulk  $^3\text{He}$  and still more at lower temperatures, a 3% error between the two measurements could cause the 4% discrepancy in pressure dependence. To avoid this error an accuracy better than 1% is required in the succeeding thermometer calibrations. The remaining discrepancy in the  $\gamma$ 's could be, for example, due to a 13% difference in the temperature scales.

In Fig. 13 we further compare our values of  $\gamma$  at zero pressure with those of Abel *et al.*<sup>36</sup> at  $P = 0.28$  bar below 30 mK. The decrease of  $\gamma$  with increasing temperature, which is seen in the data of Abel *et al.*, is clearly not present in our data between 3 and 20 mK. Our measurements do not extend above 10 mK at high pressures, where the temperature dependence of  $\gamma$  is more profound according to Abel *et al.* Obviously the extrapolation of  $\gamma$  to  $T = 0$  in the measurements of Abel *et al.* enhances the discrepancy with our data.

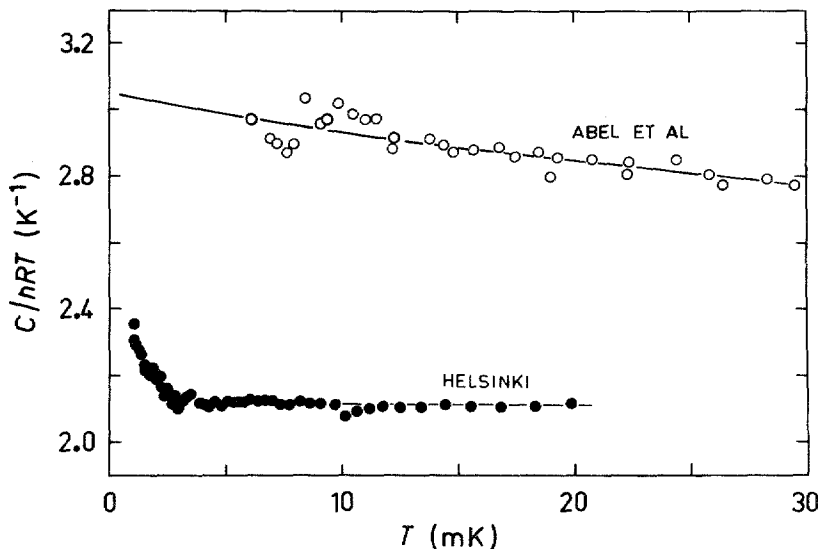


Fig. 13. A comparison of the measurements of  $\gamma$  below 30 mK near zero pressure. The data of Abel *et al.* and the smoothing by the solid line are from Ref. 36.

The measurements of Halperin *et al.*<sup>25</sup> at the melting curve result in  $\gamma = 4.33 \text{ K}^{-1}$ , which is 20% larger than our extrapolated value  $\gamma = 3.56 \pm 0.02 \text{ K}^{-1}$ . However, this difference cannot be attributed to thermometry alone. From the values of  $T_c$  and  $T_{AB}$  one can estimate that the temperature scales cause a difference less than 4% in  $\gamma$ . Since

$$\gamma = \Delta Q / (nRT \Delta T) \quad (9)$$

the remaining discrepancy must arise from inaccuracies in  $\Delta Q$  and  $n$  or in the determination of  $\Delta T$ . In our measurements the errors due to these quantities are estimated to be less than 2%, provided that our temperature scale is correct. A large systematic error could, however, be caused if part of the applied heat pulse leaked from the experimental cell, but a correction due to such an effect would further reduce our  $\gamma$ 's. If our temperature scale would turn out to be in error, Eq. (9) and the  $T_c$  curve given in Table I will facilitate a reevaluation of the  $\gamma$ 's and also the rest of Table III.

The volume derivative of the heat capacity has been recently determined by Roach *et al.*<sup>37</sup> They measured the pressure of liquid  $^3\text{He}$  at constant volume as a function of temperature and obtained the quantity  $(\partial^2 P / \partial T^2)_v$ , which is equal to  $[\partial(C_v/T) / \partial V]_T$ . From their results Roach *et al.* inferred that the heat capacity data of Ref. 35 are correct. These measurements are, however, also sensitive to the temperature scale used.

Furthermore, the heat capacity itself is not measured. Because the scatter of the data of Roach *et al.* is quite large, we believe that their evidence is weak compared to that of Ref. 26, where a direct verification of our temperature scale was made.

There is a possibility to measure the effective mass in a way which is not sensitive to the temperature scale. Rudnick<sup>38</sup> has interpreted zero sound in terms of viscoelasticity in liquid  $^3\text{He}$  and he derived an equation which related  $m^*$  to the maximum of attenuation coefficient  $\alpha$  in the transition from zero to first sound. A drawback in this method for measuring  $m^*$  is that the maximum attenuation must be measured with high absolute accuracy, since  $m^* \propto (\alpha_{\max})^{-1}$ . A fit of his theory to the zero-sound data of Abel *et al.*,<sup>39</sup> extrapolated to  $P = 0$  bar, yields 28% higher  $m^*$  than our data, while with the data of Ketterson *et al.*,<sup>40</sup> extrapolated to  $P = 30$  bar, one obtains only 12% higher  $m^*$  than our value at this pressure.

### 3.2. Discussion on the Fermi Liquid Parameters

Our values of  $\gamma$  and of the Fermi liquid parameters  $m^*/m$ ,  $F_0$ ,  $F_1$ , and  $Z_0$  will have significant theoretical implications and will necessitate reinterpretation of some experimental results. In this section we shall outline the possible changes in the physical modeling of liquid  $^3\text{He}$  based on our results.

Recent measurements of the normal fluid density  $\rho_n$  by Archie *et al.*<sup>41</sup> show a pressure-independent stripped normal fluid fraction  $\rho_n^0/\rho$  on a reduced temperature scale, indicative of large but pressure-independent strong coupling effects. This result is severely at variance with our measurements of the specific heat jump  $\Delta C/C_>$  at  $T_c$ , as will be seen in the next section. The equation employed for stripping Fermi liquid effects

$$\frac{\rho_n}{\rho} = \frac{(1 + F_1/3)(\rho_n^0/\rho)}{1 + (F_1/3)(\rho_n^0/\rho)} \quad (10)$$

is sensitive to the effective mass  $m^*/m = 1 + F_1/3$ ; the data of Ref. 35 were used in the analysis of Archie *et al.*<sup>41</sup> One can show, however, that the pressure independence of  $\rho_n^0/\rho$  will remain, if values used for  $m^*/m$  are changed by a constant factor.

Since the ratio of our  $m^*/m$  to that of Ref. 35 is constant to within 4%,  $\rho_n^0/\rho$  becomes only slightly pressure dependent by using our  $m^*/m$  in the stripping. This small dependence on  $P$  implies an order-of-magnitude smaller pressure dependence to the strong coupling effects than our measurements of  $\Delta C/C_>$ . Nevertheless, it is interesting to note that with our effective mass  $\rho_n^0/\rho$  will be close to the BCS value, indicating small strong coupling effects in contrast to the original interpretation of the data.<sup>41</sup>

Assuming  $Z_l = 0$  for  $l \geq 2$ , the contribution of the Fermi liquid molecular fields to the static spin susceptibility in the Balian-Werthamer state can be expressed in the form

$$\chi_{\text{BW}}\left(\frac{T}{T_c}\right) = \chi_n \frac{[1 + (Z_0/4)]Y(T)}{1 + (Z_0/4)Y(T)} \quad (11)$$

where  $\chi_n$  is the susceptibility of the normal liquid,  $Y(T) = \frac{2}{3} + \frac{1}{3}\Phi(T, \Delta^2)$ ,  $\Phi(T, \Delta^2)$  is the Yosida function, and  $\Delta(T/T_c)$  is the energy gap. Equation (11) should be exact in the Ginzburg-Landau region. Near  $T_c$  the trivial strong coupling corrections can be included<sup>2</sup> by multiplying  $\Delta^2(T/T_c)$  by the ratio of the observed  $\Delta C/C_>$  and the BCS value 1.43. Thus

$$\Delta\chi/\chi_n = \frac{2}{3}(1 + Z_0/4)^{-1}(\Delta C/1.43C_>)|t| \quad (12)$$

where  $\Delta\chi = \chi_n - \chi_{\text{B}}$  and  $|t| = |1 - T/T_c|$ . The nontrivial strong coupling corrections have been estimated by Serene and Rainer<sup>42</sup> to reduce the trivial corrections only by 5–10% in the *sp* approximation, the validity of which will be discussed later.

Measurements of the static susceptibility  $\chi_{\text{B}}$  by Paulson *et al.*<sup>43</sup> yielded an empirical relation  $\Delta\chi/\chi_n = 4.7|t|$  for  $|t| \leq 0.05$ , determined from the data at 20.8 bar. With the value of  $Z_0 = -2.94$  from Ref. 35 and our  $\Delta C/C_>$ , Eq. (12) gives 3.1 instead of the experimental number 4.7. The disagreement is large when compared with the experimental accuracy and the expected validity of Eq. (12). Using  $Z_0 = -3.25$  from Table III, we obtain  $\Delta\chi/\chi_n = 4.4|t|$ , in much closer agreement with experiment. However, it should be recalled that at further below  $T_c$  there is a puzzling inequality between the static and NMR measurements of  $\chi_{\text{B}}(T)$ .<sup>35</sup>

Osheroff<sup>44</sup> has found  $\chi_{\text{B}}(T)$  by NMR technique at the melting curve and Ahonen *et al.*<sup>18</sup> at  $P = 18.7$  and 29 bar. The latter measurements extend to low enough temperatures to extract  $\chi_{\text{B}}(0)/\chi_n = 0.33 \pm 0.02$ . Czerwonko<sup>45</sup> has derived the B-phase susceptibility in the form

$$\frac{\chi_{\text{B}}(0)}{\chi_n} = \frac{2}{3} \frac{1 + Z_0/4}{1 + \frac{1}{6}(Z_0 + Z_2/10)} \quad (13)$$

Using a typical value at high pressures,  $Z_0 = -3.24$ , and the result of Ahonen *et al.* for  $\chi_{\text{B}}(0)/\chi_n$ , we find from Eq. (13) that  $Z_2 = -4.6 \pm 1.4$ . This value of  $Z_2$  is unexpectedly large since one would anticipate  $F_l$  and  $Z_l$  to converge rapidly for increasing  $l$  and one generally takes  $F_l = Z_l = 0$  for  $l \geq 2$ . Near  $T_c$  the slope of the  $P = 18.7$  bar data is weaker than Eq. (12) suggests even with  $Z_0 = -2.95$  from Wheatley's tables.<sup>35</sup> However, an extrapolation of the  $P = 29$  bar data results in a much steeper slope near  $T_c$ , which is also valid for Osheroff's<sup>44</sup> results at the melting curve.

With the availability of our Fermi liquid parameters a comparison with theory at intermediate temperatures would necessitate knowing  $\Delta(T)$  and taking into account in Eq. (11) contributions from higher Fermi liquid parameters than  $Z_0$ .

There is also theoretical evidence showing that one cannot assume  $F_l = Z_l = 0$  for  $l \geq 2$  with our values of  $F_0$ ,  $F_1$ , and  $Z_0$ . The forward scattering sum rule<sup>46</sup> requires

$$\sum_{l=0}^{\infty} (A_l^s + A_l^a) = 0, \quad A_l^{a,s} = F_l^{a,s} / [1 + F_l^{a,s} / (2l + 1)] \quad (14)$$

where the notation  $F_l = F_l^s$  and  $Z_l = 4F_l^a$  is used. Assuming the parameters with  $l \geq 2$  to vanish, Eq. (14) yields, employing the values of Table III,  $F_1^a \approx 1.3$  with only a weak pressure dependence. Corruccini *et al.*<sup>47</sup> obtain  $F_1^a = -0.15 \pm 0.3$  at  $P = 0$  and  $F_1^a = 0.2 \pm 0.6$  at 27.4 bar. Reanalyzing these measurements using our values of  $F_0^a$ , one finds  $F_1^a \approx -2$  at both pressures, in contradiction with the result given by Eq. (14), assuming  $F_l = Z_l = 0$  for  $l \geq 2$ . Further using our Fermi liquid parameters and the forward scattering sum rule, and by assuming  $F_l^{s,a} = 0$  for  $l \geq 2$ , strong coupling corrections to the fourth-order Ginzburg–Landau parameters turn out divergent in the *sp* approximation.<sup>3</sup>

It should be recalled that the parameters in Table III are based on the following data: our heat capacity values of normal liquid  $^3\text{He}$  and measurements of molar volume, first sound, and magnetic temperature from Ref. 35. The above analysis is sensitive to all these data, although the heat capacity is perhaps the most difficult quantity to measure accurately owing to the problems in thermometry. We have estimated our temperature scale to be correct to 5%, and thus our results for the effective mass should be accurate within 10%.

## 4. SPECIFIC HEAT OF THE SUPERFLUID PHASES

### 4.1. Theoretical Models

The weak coupling BCS theory predicts a specific heat discontinuity at  $T_c$  of the magnitude

$$\Delta C / C_{>} = 1.43 \kappa^{-1} \quad (15)$$

where  $\Delta C = C_s(T_c) - C_n(T_c) = C_{<} - C_{>}$ . For the Balian–Werthamer (BW) state<sup>48</sup> the parameter  $\kappa = 1$  and for the Anderson–Brinkman–Morel (ABM) state<sup>49</sup>  $\kappa = 6/5$  in the weak coupling limit. The experimentally observed magnetic properties suggest that the B phase is a manifestation of the BW state and the A phase of the ABM state.

Weak coupling theory is not sufficient to describe the superfluid phases of  $^3\text{He}$  since, for example, according to it the BW state is the only stable superfluid over the whole pressure range. The corrections needed to be included in the BCS theory are called strong coupling effects; at low pressures these are presumed to be small. Consequently, one would expect  $\Delta C/C_{>} \approx 1.43$  in the B phase near  $P = 0$ . Strong coupling effects increase with increasing pressure and finally stabilize the A phase<sup>50</sup> above the polycritical point  $P_{\text{PCP}} = 21.2$  bar.

The specific heat discontinuity is perhaps the most sensitive experimentally measurable quantity to investigate strong coupling. Serene and Rainer<sup>3</sup> further propose that the temperature dependence of the specific heat in the B phase will provide a means of testing strong coupling theories, especially the weak-coupling-plus (WCP) model.

The WCP model is based on an expansion of the free energy in powers of  $T_c/T_F$ , where  $T_F$  is the Fermi temperature. The free energy functional can be written<sup>3</sup> in a form where strong coupling effects up to order  $(T_c/T_F)^3$  are accounted for by three terms. These are of the form  $\phi_{\text{sci}} \langle |t|^2 \rangle_i$ , where the temperature dependence is in the functions  $\phi_{\text{sci}}$  and  $\langle |t|^2 \rangle_i$  stands for three different averages of the quasiparticle scattering amplitude. Fortunately all  $\phi_{\text{sci}}$  have the same temperature dependence and the inadequately known scattering amplitudes define only the overall strength of strong coupling phenomena. Thus  $\Delta C/C_{>}$ , for example, may be taken as an adjustable parameter, whence the temperature dependence of the specific heat is fully determined in the WCP model. According to Serene and Rainer,<sup>3</sup> the test provided by a specific heat measurement for the WCP model applies as well to the spin fluctuation model of Brinkman *et al.*<sup>50</sup> including contributions from Refs. 51, since this model can be considered as a specific choice for the scattering amplitude within the WCP model.

Padamsee *et al.*<sup>52</sup> have introduced a model for strong coupling in which the thermodynamic properties are calculated directly from the usual expression for the entropy in a system of independent fermions, using the same quasiparticle spectrum as in the BCS theory. The energy gap  $\Delta_0$  is also in agreement with the BCS theory, except that it has been scaled by a factor chosen to produce the observed  $\Delta C/C_{>}$ . Such a scaled BCS theory accounts satisfactorily for the thermodynamics of strong coupling superconductors. The main difference between the scaled BCS theory and the WCP model is that in the latter the quantity  $(\Delta_0 - \Delta_{\text{BCS}})/\Delta_{\text{BCS}}$  reduces at low temperatures to about one-third of the value at  $T_c$ , whereas in the scaled BCS theory it is constant. This causes different initial slopes for the specific heats just below  $T_c$  when the models are adjusted to the same  $\Delta C/C_{>} \neq 1.43$ . Consequently, at high pressures the relative merits of these theories can be checked by a measurement of heat capacity near  $T_c$ , where the experimental data are most reliable.

## 4.2. Experimental Results

The specific heat of superfluid  $^3\text{He}$  varies roughly as  $T^3$  close to  $T_c$ . It is thus convenient to suppress most of the rapid temperature variation by plotting  $(C/C_{>})/(T/T_c)^3$  vs  $T/T_c$ . Such a graph is shown in Fig. 14 for four different pressures. The solid line is the result of the WCP model and the dashed line that of the scaled BCS theory. Both are adjusted to the experimental B-phase specific heat discontinuity for the appropriate pressure. Above  $P_{\text{PCP}}$  we have extrapolated the quantity  $(C_B/C_{>})/(T/T_c)^3$  linearly from  $T_{\text{AB}}$  to  $T_c$  under the thermodynamic condition

$$L = T_{\text{AB}} \int_{T_{\text{AB}}}^{T_c} (C_B - C_A) dT/T \quad (16)$$

where  $L$  is the measured latent heat at the AB transition and  $C_A$  and  $C_B$  are the heat capacities of the A and B phases, respectively; for  $C_A$  we have

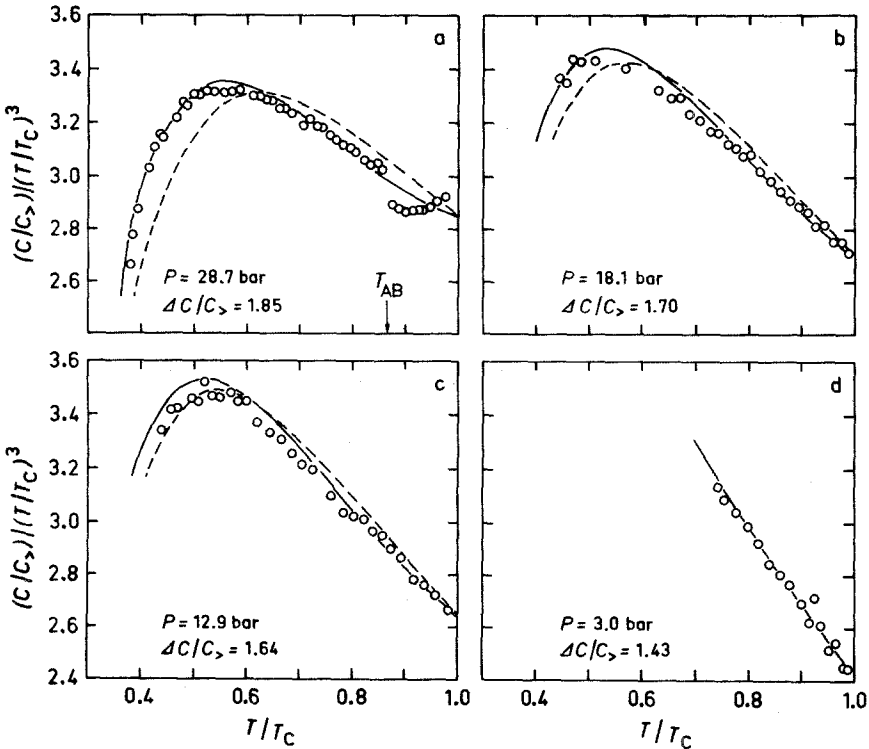


Fig. 14. Heat capacity of liquid  $^3\text{He}$  below  $T_c$  at four pressures. The solid curve follows the WCP model and the dashed line the scaled BCS theory.

used the measured values. Equation (16) results from the requirement that the entropies of both phases are equal at  $T_c$  and differ by  $L/T_{AB}$  at  $T_{AB}$ .<sup>35</sup>

A general feature of our high-pressure data is that they agree much better with the WCP model than with the scaled BCS theory. Since  $\Delta C/C_>$  is used as a fitting parameter in the theories, the agreement above  $P_{PCP}$  depends on the manner in which the extrapolation of the B-phase data is done from  $T_{AB}$  to  $T_c$ . Nevertheless, the above conclusion about the agreement remains valid even if the WCP model or the scaled BCS theory, alternatively, were used for the temperature dependence of  $C_B$  between  $T_{AB}$  and  $T_c$ . At 28.7 bar, for example, the linear extrapolation yields  $\Delta C/C_> = 1.85$  using Eq. (16) when  $C_B(T_{AB})$  is fixed to the experimental value. The corresponding numbers using  $C_B$  of the WCP model or of the scaled BCS theory yield 1.87 and 1.82, respectively, when  $\Delta C/C_>$  itself is used as an adjustable parameter in Eq. (16). However, using  $\Delta C/C_> = 1.87$  in the WCP model we find that the agreement of this theory with the data is as good as in Fig. 14a, while with  $\Delta C/C_> = 1.82$  the scaled BCS theory remains incompatible with the data below  $T_{AB}$ . At low pressures strong coupling effects diminish and, consequently, the two theories approach the BCS result as well as the experimental data.

Below  $T/T_c \approx 0.5$  the good agreement between the WCP model and the experimental data shown in Fig. 14a could be accidental. At these temperatures a plot of this type is quite sensitive to systematic errors, for instance, in the background heat capacity or in the temperature scale. Such errors tend to vanish near  $T_c$ . We may thus conclude that the WCP model works well at least near  $T_c$ .

In the A phase the temperature dependence of the heat capacity at different pressures is qualitatively similar to that shown in Fig. 14a. The relative difference  $(C_A - C_B)/\frac{1}{2}(C_A + C_B)$  at  $T_{AB}$  appears to be roughly of the same magnitude but of opposite sign as at  $T_c$ . Because  $C_A = C_B$  at a temperature much closer to  $T_c$  than to  $T_{AB}$ , at least at pressures well above  $P_{PCP}$  the difference  $C_A - C_B$  cannot be strictly linear in  $T$  between  $T_{AB}$  and  $T_c$  as suggested by measurements of Paulson *et al.*<sup>53</sup> near PCP. Since the WCP model reproduces  $C_B$  satisfactorily, one would also like to have an estimate for  $C_A$  in this model. A detailed comparison with experiments could give new information about the scattering amplitude.

In Fig. 15 we have plotted the specific heat discontinuity  $\Delta C/C_>$  vs pressure. Above  $P_{PCP}$  the value of  $C_<$  for the B phase is determined by a linear extrapolation of  $(C_B/C_>)/(T/T_c)^3$  from  $T_{AB}$  to  $T_c$  and by requiring Eq. (16) to be valid. If, instead, the WCP model were used for  $C_B$  in the extrapolation, the B-phase points at  $P = 28.7$  and 32.5 bar would increase by 1%. The correction in  $\Delta C/C_>$  due to the volume  $V_n$  filled with normal  $^3\text{He}$  in the sinter is roughly proportional to  $V_n/V$ , where  $V$  is the free

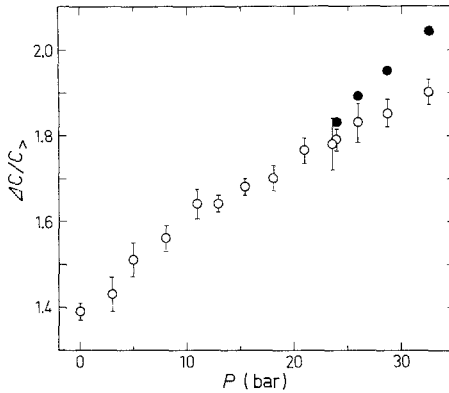


Fig. 15. The specific heat discontinuity  $\Delta C/C_>$  vs pressure. Open and filled circles are data for the B and A phases, respectively. The error bars are due to extrapolations of  $C_>$  and  $C_<$ ; for the A phase they are the same as for the B phase at the same pressure.

volume of the cell. If  $V_n$  should not be scaled by  $\xi_0$  as described in Section 2.4, the values of  $\Delta C/C_>$  would be 2–3% larger than those shown in Fig. 15 at highest pressures.

For  $P \leq 10$  bar, the excess specific heat observed in the normal liquid near  $T_c$  causes some ambiguity when comparing the measured discontinuity with the BCS result. At zero pressure  $\Delta C/C_> = 1.39 \pm 0.02$ , while  $\Delta C/nR\gamma T_c = 1.52$  and  $(C_< - nR\gamma T_c)/nR\gamma T_c = 1.61$ . The right interpretation is  $\Delta C/nR\gamma T_c$  if the excess is due to a surface effect or to a background. The latter quantity should be applied only when superfluidity quenches the excess heat capacity. However, the requirement that the entropies of the normal and superfluid phases should be equal at  $T_c$  suggests that the excess continues below  $T_c$ . Both  $\Delta C/nR\gamma T_c$  and  $(C_</math>  $/nR\gamma T_c - 1)$  display an unexpected minimum at  $P \approx 3$  bar. Consequently we have assumed that  $\Delta C/C_>$  should be used in studying strong coupling effects.$

For the B phase at zero pressure  $\Delta C/C_>$  is close to the BCS value 1.43. An extrapolation of  $\Delta C/C_>$  to the melting curve yields  $\Delta C/C_> = 1.92 \pm 0.04$  for the B phase and  $2.08 \pm 0.04$  for the A phase; the corresponding numbers from Ref. 6 are  $1.90 \pm 0.08$  and  $2.00 \pm 0.08$ , respectively. Webb *et al.*<sup>4</sup> obtain systematically 15–20% lower  $\Delta C/C_>$  than we in the A phase. However, the pressure slope of  $\Delta C/C_>$  in their data is approximately equal to ours. The measurements of Andres and Darack<sup>8</sup> show slightly smaller values of  $\Delta C/C_>$  than our data at all pressures. The precision

of their results is too poor to enable a reasonable comparison of the pressure dependences.

In contrast to the measurements by Archie *et al.*,<sup>41</sup> our data demonstrate a clear pressure dependence of strong coupling effects. This difference could be caused by the nontrivial strong coupling effects, in the terminology of Serene and Rainer.<sup>42</sup> They estimate such effects to be small in the *sp* approximation, using Fermi liquid parameters of Ref. 35 and by employing the forward scattering sum rule of Eq. (14). However, with our values of the Fermi liquid parameters the calculated specific heat discontinuity diverges in the *sp* approximation at high pressures.<sup>3</sup> Consequently, there is ample reason to take this approximation cautiously.

## 5. LATENT HEAT AT THE AB TRANSITION

The Clausius–Clapeyron equation relates the slope of the transition pressure  $dP/dT$  and the volume change  $\Delta V$  at a first-order transition to latent heat by

$$L = \Delta V T dP/dT \quad (17)$$

In the AB transition of superfluid  $^3\text{He}$ ,  $\Delta V$  is so small that the pressure change in a constant-volume process is negligible. Thus no special arrangements are needed to retain constant pressure during the transition.

We observed the  $B \rightarrow A$  transition as a plateau in the temperature drift curve. The  $A \rightarrow B$  transition was supercooled and could be observed as a heat pulse of magnitude  $L$ . Since the  $B \rightarrow A$  transition proceeded at constant temperature and was reproducible to high accuracy,  $\pm 0.5 \mu\text{K}$ , we conclude that B liquid could not have been significantly superheated. A typical behavior of temperature in the  $B \rightarrow A$  transition is shown in Fig. 16. The average  $T$  in the plateau region is taken to be the transition temperature  $T_{AB}$  as mentioned in Section 3.

The latent heat was determined from the heat leak  $\dot{Q}$  to the sample and the duration  $\Delta t$  of the transition;  $L = \dot{Q} \Delta t$ . The heat leak was obtained from the temperature drift curve  $\dot{T}$  and the total heat capacity  $C$ , using  $\dot{Q} = C\dot{T}$ . The background heat capacity is negligibly small at  $T_{AB}$  and thus it will not cause a notable error, even if the temperature of the background did not stay at  $T_{AB}$  during the transition. An alternative method, based on a comparison of  $\dot{T}$  caused by the residual heat leak and an additional external heat leak, yielded the same  $\dot{Q}$  as the above method within the precision of our measurements. An accuracy of  $\pm 0.02 \mu\text{J}/\text{mole}$  was achieved in determining  $L$ .

The molar latent heat  $L/n$  at  $T_{AB}$  is plotted vs  $P$  in Fig. 17. The pressure of the polycritical point  $P_{PCP} = 21.22 \text{ bar}$ , shown by an arrow, is

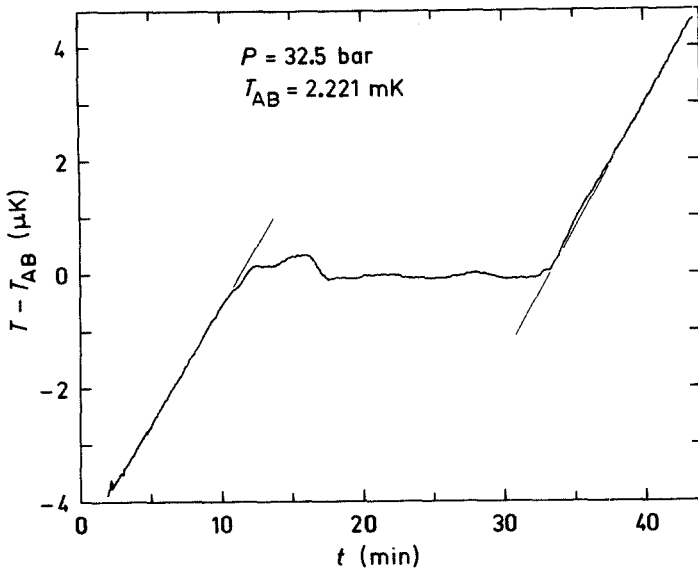


Fig. 16. The temperature drift vs time for the B  $\rightarrow$  A transition at 32.5 bar.

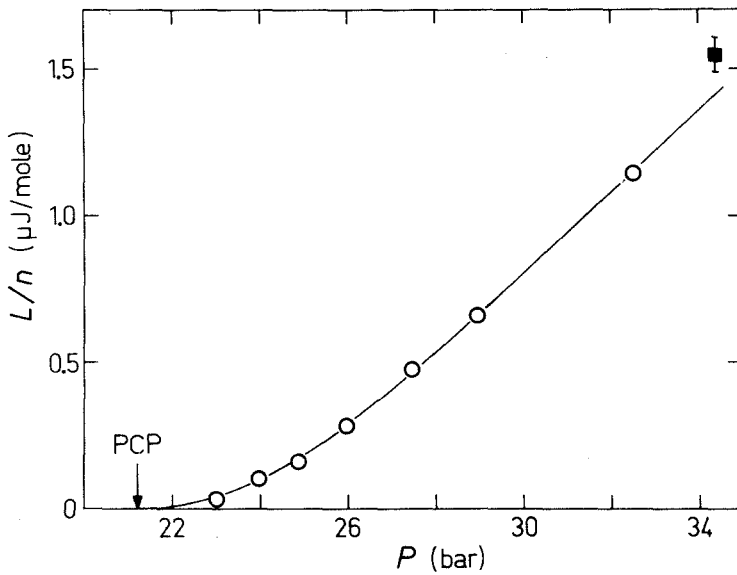


Fig. 17. The molar latent heat at  $T_{AB}$  vs pressure measured at zero magnetic field. The arrow indicates the polycritical point. Open circles are our measurements and the filled square is from Halperin *et al.*<sup>25</sup> at the melting curve.

determined by Paulson *et al.*<sup>53</sup> Our  $P$  vs  $T_{AB}$  data seem to intersect the  $T_c$  line at a higher pressure, about 21.5 bar. Since the entropy difference between the A and B phases vanishes at  $P_{PCP}$ ,  $L$  must extrapolate to zero at the polycritical point, which is also clear from Fig. 17. At  $P = 23.0$  bar,  $L/n$  is only  $0.03 \pm 0.02 \mu\text{J}/\text{mole}$ , while at 32.5 bar,  $L/n = 1.14 \pm 0.02 \mu\text{J}/\text{mole}$ . Our resolution did not allow a reliable observation of the  $B \rightarrow A$  transition below 23 bar. Halperin *et al.*<sup>25</sup> have found  $L/n = 1.54 \pm 0.06 \mu\text{J}/\text{mole}$  at the melting curve, which differs by less than 10% from our extrapolated value.

Equation (17) can be used to estimate the change of volume in the AB transition. At 32.5 bar we obtain  $\Delta V_{AB} = +1.1 \times 10^{-7} \text{ cm}^3$ , which corresponds at constant pressure and volume to a negligible transfer of liquid  $^3\text{He}$  through the filling capillary.

## 6. SUMMARY

We have measured the specific heat of liquid  $^3\text{He}$  in zero magnetic field from 0.8 to 10 mK and at pressures from 0 to 32.5 bar.

For thermometry we employed the magnetic susceptibility of CLMN. The high resolution of this thermometer, better than one part in  $10^4$ , allowed 1% precision in our heat capacity data. The CLMN susceptibility was calibrated by means of platinum NMR thermometry using the Korringa relation  $\tau_1 T = 29.9 \text{ msec K}$ . We estimate the absolute accuracy of our temperature scale to be  $\pm 5\%$ ; the error limits are mainly caused by uncertainties in the value of  $\tau_1 T$ .

For the critical temperature of the second-order transition we find  $T_c = 1.04 \text{ mK}$  at  $P = 0$  and  $T_c = 2.79 \pm 0.02 \text{ mK}$  at the melting curve by extrapolation from lower pressures. Our magnetic temperatures and those of the La Jolla group,<sup>21</sup> also determined with a CLMN thermometer, are proportional to each other and obey  $T_{LJ}^* = 0.9 T_{\text{Hki}}^*$  to within  $\pm 5 \mu\text{K}$ . The calibration with our platinum NMR thermometer reveals that to obtain absolute temperatures a constant  $\Delta$  of about 0.1 mK must be subtracted from our magnetic temperatures, while the La Jolla group<sup>21</sup> estimates  $\Delta$  to be of the same magnitude but of the opposite sign.

The background heat capacity of our experimental cell was carefully determined from a series of measurements at zero pressure with variable amounts of liquid  $^3\text{He}$  in the cell. Since the background is negligible at high pressures near and above  $T_c$ , we have assumed that it is independent of  $P$ . A correction due to  $^3\text{He}$  remaining as normal liquid below  $T_c$  at the sinter surfaces within the superfluid coherence length was taken into account, as suggested by measurements at zero pressure.

The specific heat of normal  $^3\text{He}$  is proportional to temperature within the precision of our measurements ( $\pm 1\%$ ), except for lowest pressures below 3 mK, where an excess specific heat was observed. This excess is about 9% at  $T_c$  and at  $P=0$  and it decreases with increasing pressure; at 8 bar it is negligible. The excess specific heat is, most likely, an intrinsic property of bulk liquid  $^3\text{He}$ , because a surface effect would require a characteristic length of a few hundred micrometers, much longer than the quasiparticle mean free path or the range of the surface potential.

The effective mass of  $^3\text{He}$  was determined from the specific heat of the normal liquid, excluding the data that exhibit the excess heat capacity. The previously accepted values of  $m^*/m$ , compiled in Ref. 35 by Wheatley, are about 40% larger than ours. This suggests considerable revisions to the calculated Fermi liquid parameters  $F_0$ ,  $Z_0$ , and  $F_1$ . It must be recalled, however, that the values of  $m^*/m$  are sensitive to the temperature scale used. For example, if our scale were to be corrected by a constant factor  $A$ , the effective mass should be multiplied by  $A^{-2}$ . We estimate the possible correction due to the temperature scale to be less than 10% in the effective mass.

The temperature dependence of the specific heat in the B phase agrees with the weak-coupling-plus model of Serene and Rainer.<sup>3</sup> The relative difference  $(C_A - C_B)/\frac{1}{2}(C_A + C_B)$  at  $T_{AB}$  and  $T_c$  appears to be roughly of equal magnitude but of opposite sign.

We observe a clear pressure dependence of strong coupling effects as measured by the specific heat discontinuity  $\Delta C/C_>$  at  $T_c$ ; for zero pressure we find  $\Delta C/C_> = 1.39 \pm 0.02$ , quite close to the BCS result 1.43. Our extrapolated values of  $\Delta C/C_>$  at the melting curve are  $2.08 \pm 0.04$  in the A phase and  $1.92 \pm 0.04$  in the B phase, in agreement with the measurements of Halperin *et al.*,<sup>6</sup> who find  $2.00 \pm 0.08$  and  $1.90 \pm 0.08$  for the A and B phases, respectively.

Due to the large sample volume and the high resolution of the CLMN thermometer, we could measure calorimetrically the latent heat of the B  $\rightarrow$  A transition. At 32.5 bar,  $L = 1.14 \pm 0.02 \mu\text{J}/\text{mole}$  and it decreases quickly toward PCP as expected on thermodynamic grounds.

As a conclusion, we can assert that the present low-temperature techniques permit a precision better than 1% in a measurement of  $^3\text{He}$  heat capacity at millidegree temperatures. The final accuracy is mainly restricted by the temperature scale.

### ACKNOWLEDGMENTS

The authors are indebted to L. Östman, J. Ray, T. Soenne, and especially to P. Main for their contributions at various stages of these

measurements. Useful conversations with A. Ahonen, H. Collan, J. Kurkijärvi, O. Lounasmaa, D. Osheroff, D. Rainer, M. Salomaa, J. Wheatley, and J. Wilkins are gratefully acknowledged.

## REFERENCES

1. G. Baym and C. J. Pethick, in *The Physics of Liquid and Solid Helium*, K. H. Bennemann and J. B. Ketterson, eds. (Wiley, New York, 1978), Vol. II, Chapter 1, and references therein.
2. A. J. Leggett, *Rev. Mod. Phys.* **47**, 331 (1975); P. W. Anderson and W. F. Brinkman, in *The Physics of Liquid and Solid Helium*, K. H. Bennemann and J. B. Ketterson, eds. (Wiley, New York, 1978); Vol. II, Chapter 3.
3. D. Rainer and J. W. Serene, *Phys. Rev. B*, **13**, 4745 (1976); J. W. Serene and D. Rainer, *J. Low Temp. Phys.* **34**, 589 (1979).
4. R. A. Webb, T. J. Greytak, R. T. Johnson, and J. C. Wheatley, *Phys. Rev. Lett.* **30**, 210 (1973).
5. J. M. Dundon, D. L. Stofa, and J. M. Goodkind, *Phys. Rev. Lett.* **30**, 843 (1973).
6. W. P. Halperin, C. N. Archie, F. B. Rasmussen, T. A. Alvesalo, and R. C. Richardson, *Phys. Rev. B* **13**, 2124 (1976).
7. S. E. Shields and J. M. Goodkind, *J. Low Temp. Phys.* **27**, 259 (1977).
8. K. Andres and S. Darack, *Physica (Utrecht)* **86-88B**, 1071 (1977); K. Andres (Bell Laboratories), private communication.
9. D. O. Edwards, J. D. Feder, W. J. Gully, G. G. Ihas, J. Landau, and K. A. Muething, *J. Phys. (Paris)* **39**, C6-260 (1978).
10. T. A. Alvesalo, T. Haavasoja, P. C. Main, M. T. Manninen, J. Ray, and Leila M. M. Rehn, *Phys. Rev. Lett.* **43**, 1509 (1979); T. A. Alvesalo, T. Haavasoja, M. T. Manninen, and A. T. Soinnie, *Phys. Rev. Lett.* **44**, 1076 (1980).
11. T. A. Alvesalo, T. Haavasoja, P. C. Main, L. M. Rehn, and K. M. Saloheimo, *J. Phys. (Paris) Lett.* **39**, L-459 (1978).
12. O. V. Lounasmaa, *Experimental Principles and Methods Below 1 K* (Academic Press, New York, 1974).
13. M. C. Veuro, Ph.D. Thesis, Acta Polytechnica Scandinavica, Ph. 122 (1978).
14. H. R. O'Neal and N. E. Phillips, *Phys. Rev.* **137**, A748 (1965).
15. E. R. Grilly, *J. Low Temp. Phys.* **4**, 615 (1971).
16. V. N. Grigor'ev, B. N. Yesel'son, V. A. Mikheev, and O. A. Tolkacheva, *Zh. Eksp. Teor. Fiz.* **52**, 871 (1967) [*Sov. Phys.—JETP* **25**, 572 (1967)].
17. M. I. Aalto, H. K. Collan, R. G. Gylling, and K. O. Nores, *Rev. Sci. Instr.* **44**, 1075 (1973).
18. A. I. Ahonen, M. Krusius, and M. A. Paalanen, *J. Low Temp. Phys.* **25**, 421 (1976).
19. E. Varoquaux, *J. Phys. (Paris)* **39**, C6-1605 (1978).
20. D. O. Edwards, J. D. Feder, W. J. Gully, G. G. Ihas, J. Landau, and K. A. Muething, in *Physics at Ultralow Temperatures* (Proc. Internat. Symp. Hakoné 1977) (Phys. Society of Japan, 1978).
21. D. N. Paulson, M. Krusius, J. C. Wheatley, R. S. Safrata, M. Koláč, T. Těthal, K. Svec, and J. Matas, *J. Low Temp. Phys.* **34**, 63 (1979); **36**, 721 (E) (1979).
22. M. I. Aalto, H. K. Collan, R. G. Gylling, and K. O. Nores, *Phys. Lett.* **41A**, 469 (1972), and references therein.
23. O. Avenel, M. Bernier, D. Bloyet, P. Piéjus, E. Varoquaux, and C. Vibet, in *Low Temperature Physics—LT 14*, M. Krusius and M. Vuorio, eds. (North-Holland, Amsterdam, 1975); Vol. IV, p. 64.
24. P. M. Berglund, H. K. Collan, G. J. Ehnholm, R. G. Gylling, and O. V. Lounasmaa, *J. Low Temp. Phys.* **6**, 357 (1972).
25. W. P. Halperin, F. B. Rasmussen, C. N. Archie, and R. C. Richardson, *J. Low Temp. Phys.* **31**, 617 (1978).

26. E. Lohta, M. T. Manninen, J. P. Pekola, A. T. Soenne, and R. J. Soulen, Jr. *Phys. Rev. Lett.* **47**, 590 (1981).
27. R. J. Soulen, Jr., and H. Marshak, *Cryogenics* **22**, 408 (1980).
28. B. Hébral, G. Frossati, H. Godfrin, G. Schumacher, and D. Thoulouze, *J. Phys. (Paris) Lett.* **40**, L-41 (1979).
29. M. T. Béal-Monod (Université de Paris-Sud), to be published.
30. W. F. Brinkman and S. Engelsberg, *Phys. Rev.* **169**, 417 (1968).
31. S. Doniach and S. Engelsberg, *Phys. Rev. Lett.* **17**, 750 (1966).
32. D. J. Amit, J. W. Kane, and H. Wagner, *Phys. Rev. Lett.* **19**, 425 (1967).
33. J. M. Parpia, D. J. Sandiford, J. E. Berthold, and J. D. Reppy, *Phys. Rev. Lett.* **40**, 565 (1978).
34. J. Jaffe, *J. Low Temp. Phys.* **37**, 567 (1979).
35. J. C. Wheatley, *Rev. Mod. Phys.* **47**, 415 (1975).
36. W. R. Abel, A. C. Anderson, W. C. Black, and J. C. Wheatley, *Phys. Rev.* **147**, 111 (1966).
37. P. R. Roach, Y. Eckstein, and M. W. Meisel, *Physica* **108B+C**, 1211 (1981).
38. Isadore Rudnick, *J. Low Temp. Phys.* **40**, 287 (1980).
39. W. R. Abel, A. C. Anderson, and J. C. Wheatley, *Phys. Rev. Lett.* **17**, 74 (1966).
40. J. B. Ketterson, P. R. Roach, B. M. Abraham, and P. D. Roach, in *Quantum Statistics and the Many Body Problem*, S. B. Trickey, W. P. Kirk, and J. W. Dufty, eds. (Plenum Press, New York, 1975), p. 35.
41. C. N. Archie, T. A. Alvesalo, J. D. Reppy, and R. C. Richardson, *Phys. Rev. Lett.* **43**, 139 (1979); *J. Low Temp. Phys.* **42**, 295 (1981).
42. J. W. Serene and D. Rainer, *Phys. Rev. B* **17**, 2901 (1978).
43. D. N. Paulson, H. Kojima, and J. C. Wheatley, *Phys. Lett.* **47A**, 457 (1974).
44. D. D. Osheroff, *Phys. Rev. Lett.* **33**, 1009 (1974).
45. J. Czerwonko, *Acta Phys. Pol.* **32**, 335 (1967).
46. N. D. Mermin, *Phys. Rev.* **159**, 161 (1967).
47. L. R. Corruccini, D. D. Osheroff, D. M. Lee, and R. C. Richardson, *J. Low Temp. Phys.* **8**, 229 (1972).
48. R. Balian and N. R. Werthamer, *Phys. Rev.* **131**, 1553 (1963).
49. P. W. Anderson and W. F. Brinkman, *Phys. Rev. Lett.* **30**, 1108 (1973).
50. W. F. Brinkman, J. W. Serene, and P. W. Anderson, *Phys. Rev. A* **10**, 2386 (1974).
51. Y. Kuroda, *Prog. Theor. Phys.* **53**, 349 (1975); L. Tewordt, D. Fay, P. Dorre, and D. Einzel, *Phys. Rev. B* **11**, 1914 (1975); L. Tewordt, D. Fay and N. Schopohl, *J. Low Temp. Phys.* **30**, 177 (1978).
52. H. Padamsee, J. E. Neighbor, and C. A. Shiffman, *J. Low Temp. Phys.* **12**, 387 (1973).
53. D. N. Paulson, M. Krusius, and J. C. Wheatley, *J. Low Temp. Phys.* **25**, 699 (1976).